Original Research Article

Battery management of photovoltaic-based standalone DC microgrid for houses in rural areas

ABSTRACT

DC Microgrids are very popular these days because they can provide qualitative and quantitative energy to remote regions. There is stochastic behaviour and uncertainty in DC microgrids (MG) that use renewable resources. As a result, battery units are required in DC microgrids to assure power balance. Effective coordination and control are necessary for standalone DC MG to accomplish efficient energy management and effective utilization of resources and storage units. A 48V standalone DC MG for remote residences is proposed, consisting of a photovoltaic (PV) system, MPPT, DC/DC boost converters, and storage batteries. Only a few of the challenges include the integration of distributed energy resources (DERs) into DC MG, MPPT, battery charge-discharge control, and voltage deviation control at the DC bus. All of these issues have been considered and investigated in this paper. As a result, the existence of a complete control platform is highly desirable. The entire system is created and tested in the Typhoon Hil environment.

Keywords: DC microgrid, battery, state of charge, Maximum power point, DC-DC converters

1. INTRODUCTION

MG is described as "a group of interconnected loads and dispersed energy resources inside clearly defined electrical boundaries that works as a single controllable entity concerning the grid" by the Department of Energy (DoE). To operate a microgrid in both grid-connected and island mode, a point of common coupling (PCC) is used that can connect and disconnect the microgrid from the grid. Currently installed AC PV MGs use PV to generate DC power, which is then inverted to AC through a grid-tied inverter and then converted back to DC on the load side. DC/AC conversion on the PV side and AC/DC conversion on the DC load side are both necessary energy conversion processes for this AC power system. A significant and growing percentage of loads use DC power and renewable energy sources like solar and fuel cells provide DC power. DC-DC converters are required to install a DC network connecting DC loads to DC sources [1]–[4].

A simplified schematic of a general DC MG with batteries, DC-DC converters, different types of loads, and solar panels as the energy source is depicted in **Fig 1**.

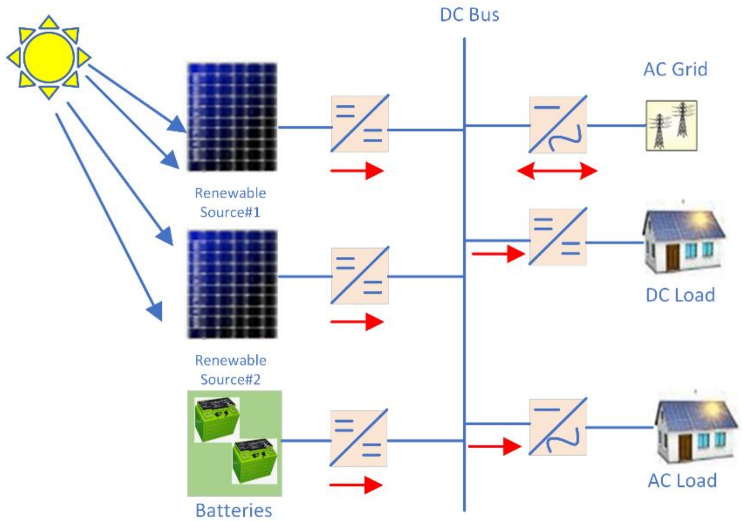

Fig 1. Structure of DC MG

There are several difficulties in designing such a DC MG. One of the key challenges is to keep the losses low, otherwise, it would not be very different from the AC MG. The Photovoltaic source is intermittent. So, it is quite challenging to obtain a constant power supply from these types of sources [5]–[10]. During the day, PV panel voltage at a maximum power point (MPP) varies. The voltage of the battery varies based on its state of charge (SOC), but the load is required to run at a constant voltage. As a result, the design would necessitate some sophisticated power electronics in order for the solar PV to work at its MPP and the battery to be charged and drained optimally while driving the load with minimal losses [11]. This issue can be resolved by using an MPPT controller, proper battery management, and closed-loop converters. Converters act as an interface between the load, the battery, and the PV panel [12].

A 48V DC MG is presented in this research to power rural households utilizing PV panels and batteries connected to a dc power line of 48V. The system is having photovoltaic source with an MPPT controller, boost converters with inner loops, and storage batteries with SOC management. The considerable variability of PV systems' output power is one of their most distinguishing features. Because these systems are static, any change in the irradiance reaching the PV arrays results in a commensurate change in their output power. There is a lot of stochastic behavior and uncertainty in DC microgrids that use renewable energy. As a result, at the generation stage of DC microgrids, BESSs, which comprise battery units and their controllers, are used to assure power balance. Furthermore, more than one BESS is required to make the system redundant [13]. When more than one BESS is used in a DC microgrid, however, there is a risk that one of the batteries will be exposed to deep draining or overcharging without being able to manage it.

So, the performance of the MPPT controller to harness maximum power from PV sources, controller for a storage battery, and voltage controller for converters to maintain reference output voltage with acceptable values is analyzed by Typhoon Hil software.

2. SYSTEM STRUCTURE

Fig 2 depicts the system under consideration, which consists of a PV source connected to DC load through two batteries and dc-dc converters. There is no need to put an additional controller to switch the system from MPPT mode to bus regulation mode and vice versa. This is made possible by battery management based on battery SOC. The use of two batteries in the system solves two purposes.

- To make the battery storage system redundant and smooth operation of MPPT and bus voltage regulation modes.
- DC-DC converters will be having constant input voltage most of the time and the circulating current is zero if line resistance is the same for two sources to be connected in parallel.

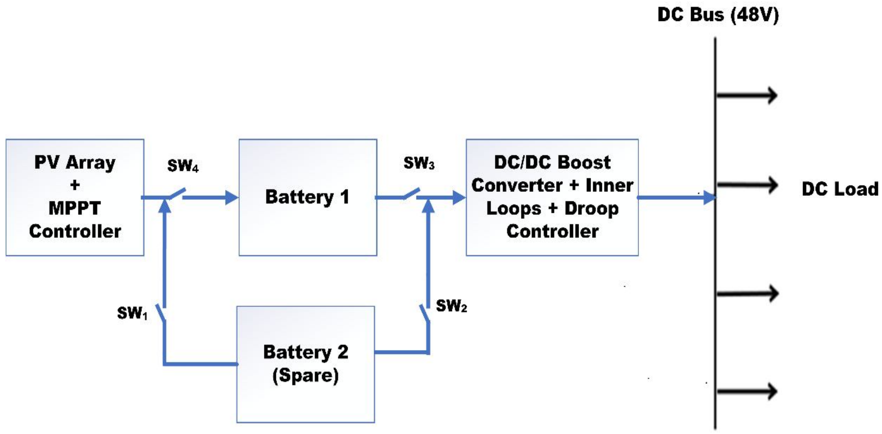

Fig 2. Block diagram of system chosen

2.1 MAXIMUM POWER POINT CONTROLLER

With PV systems, MPPT is a technology that is utilized to maximize power extraction under all circumstances. In this research, perturb and observe algorithm is used for maximum power extraction. This algorithm continuously matches the load impedance with the arbitrary impedance of the PV module with the aid of an appropriate converter. As its name implies, an effective MPPT algorithm can search and locate the MPP of a nonlinear electrical generator regardless of the ambient weather. In this instance, PV sources are nonlinear electric generators. The MPPT algorithm must function despite very changeable weather conditions at all times when all PV panels make up a source for its MPP. The MPPT strategy aims to find the voltage or current at which the PV system provides the maximum output power.

A PV cell can function at a variety of voltages (V) and currents (I). The maximum power point (MPP) can be found by gradually raising a cell's voltage from minimum to its maximum value. The critical point is reached when the cell produces the peak electrical power possible with the level of radiation it has received. An algorithm may utilize the following equation to determine the MPP:

$$P_{PV}(t) = V_{PV}(t) \cdot I_{PV}(t) \quad (1)$$

Equation (1) can be differentiated with respect to voltage VPV as follows:

$$\frac{dP_{PV}}{dV_{PV}} = I_{PV}(t) + V_{PV}(t) \cdot \frac{dI_{PV}}{dV_{PV}} \tag{2}$$

and at the MPP:

$$\frac{dP_{PV}}{dV_{PV}} = 0 \tag{3}$$

$$\frac{dI_{PV}}{dV_{PV}} = -\frac{I_{PV}}{V_{PV}} \tag{4}$$

As a result, the algorithm searches for the location where the conductance (I_{PV}/V_{PV}) and the conductance increment (dI_{PV}/dV_{PV}) are identical. Four significant quantities; short-circuit current (ISC), open-circuit voltage (VOC), current at the MPP (Imp), and voltage at the MPP (Vmp) make up the **I** (V) characteristic shown in **fig 3**.

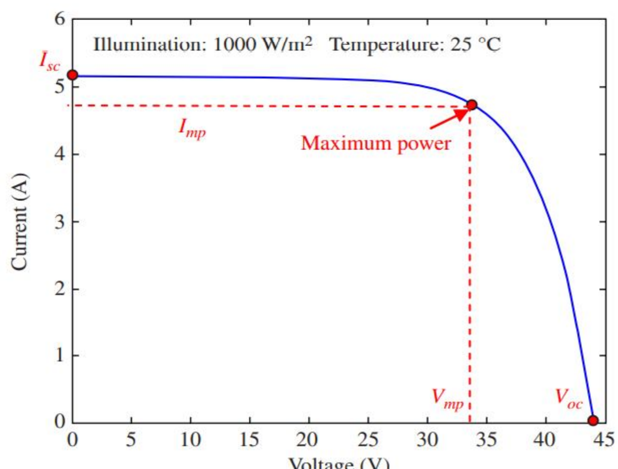

Fig 3. I (V) Characteristic of a PV panel

2.2 CHARGE/DISCHARGE CONTROL OF BATTERIES

Storage units are managed based on power generation, SOC of batteries, and load demand. SOC of batteries is regulated by controlling the switches to limit the charge-discharge currents. During day time, perturb and observe algorithm is implemented to extricate maximum power from the PV panel. A backup battery is incorporated with DC MG to execute power-sharing based on various conditions such as demand, availability of solar power, and temperature According to the battery SOC, the sequential operation of batteries in DC MG during day/sunny time is explained by the flow chart as shown in **fig. 3** and night/rainy time is explained by the flow chart as shown in **fig. 4**. SOC_1 is the state of charge of battery 1 (main battery), SOC_2 is the state of charge of battery 2 (spare battery). Management strategy is explained with respect to SOC_1.

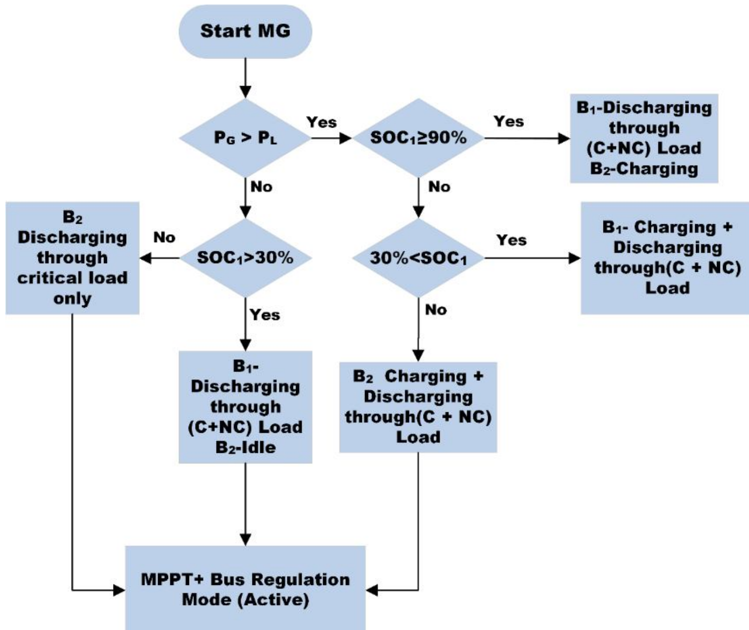

Fig 4. Flow Chart of battery management during a sunny day

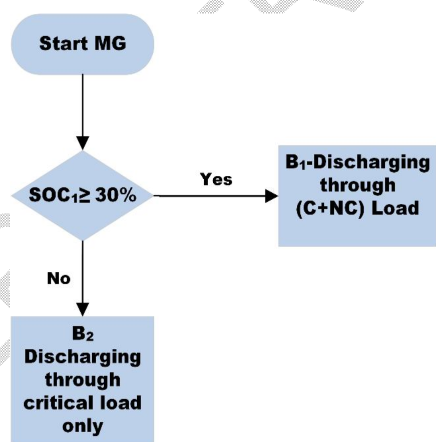

Fig 5. Flow Chart of battery management during rainy day/night time

Fig. 5 shows the division of the operation into five zones as per the load power demand and supply. Operating switches make the standalone DC MG system shift from one zone to another which connects the DC load, source, and storage system as needed. Region 1 and Region 2 indicate the operation of both batteries during daytime and night time respectively. Following the battery 1 SOC threshold, the functioning of each zone will take place.

Zone 1. When source power is more than load demand (during sunny/day time) and SOC_1 is more than 90% percent, at the same time, the solar panel does a dual action i.e charges the backup battery B_2 and transmits the power to load.

Zone 2. In the afternoon, when SOC_1 is more than 30% and there is a demand for peak load, battery B_1 charges discharges simultaneously to fulfill the demand.

Zone 3. The spare battery for emergency purposes will start charging, and discharging simultaneously whenever SOC_1 is below 30% and demand is more than source power.

Zone 4. Solar power is not accessible in the evening. As long as, SOC_1 is more than 30%, power is transferred to critical and non-critical loads through B_1.

Zone 5. As SOC_1 is less than 30%, B_2 will start discharging to supply power to the critical load.

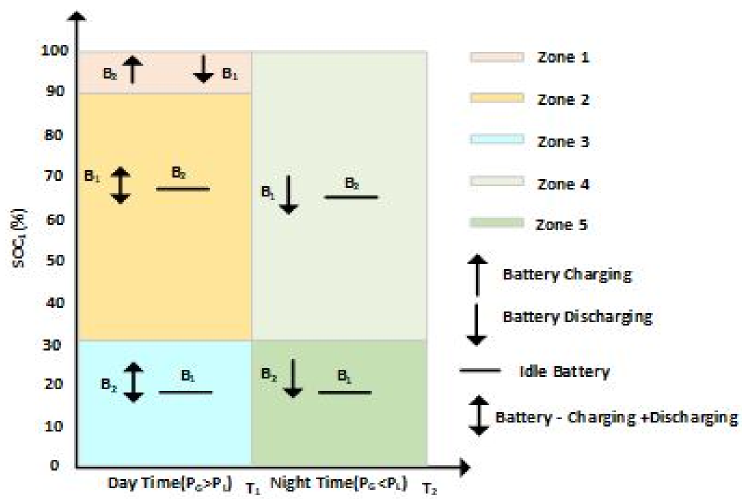

Fig. 6 Zonewise operation of batteries

3. RESULTS AND DISCUSSION

Simulation of the system shown in **fig. 2** is carried out in Typhoon Hil environment. Simulation outcomes for various circumstances are demonstrated in this part. A DC-DC boost converter with inner loops is used. To give a reference value, the voltage control loop is used. Specifications of system components like PV, battery, boost converters are given in **Table 1.**

3.1 MPPT controller

An effective maximum power point tracking (MPPT) system is required to raise solar photovoltaic (PV) panel efficiency. In this paper perturbation and observation (P&O) algorithm is used to track maximum power. Simulations are performed using Typhoon Hil software for tracking MPPs of the solar PV panel. Maximum output power from the solar PV panel is provided at an MPP with V_{MPP} and I_{MPP}. The MPP is determined at the standard test conditions (STC) of the irradiation, 1 kW/m^2, and module temperature, 25^{0}C, however, these conditions are seldom met. **Fig. 7** shows the V-I and V-P characteristics of the solar PV panel at STC. **Fig 8(a)** and **7(b)** show V-I, and V-P characteristics for irradiation of 800 watt/m^2 and 600 watt/m^2 at 25^{0}C respectively. **Fig 9(a)** and **8(b)** show V-I, and V-P characteristics for a temperature of 30^{0}C and 35^{0}C at 1000 watts of irradiation respectively. **Fig. 7–9** demonstrate how changes in temperature and irradiation have an impact on the output voltage and current. However, there is a certain maximum point on the V-I or V-P curve, at which the solar PV panel functions with maximum efficiency and generates maximum output power, regardless of the meteorological conditions.

TABLE I: Parameters for Simulation in Standalone DC MG

Parameters	Symbol	Value
Bus Voltage (Nominal)	V_{bus}	48 V
Maximum PV Power @ 1000 W/m^2, 25°C	P_m	186 W
Open circuit voltage	V_{oc}	41V
Short Circuit Current	I_{sc}	5.6A
Battery Nominal Voltage	V	36V
Battery Capacity	AH	10 AH
Converter Switching Frequency	f_{sw}	10kHz
Filter Inductor	L	3e-3H
Filter Capacitor	C	810e-6F
Filter inductor ESR	r_L	0.1Ω
Filter capacitor ESR	r_C	0.001Ω

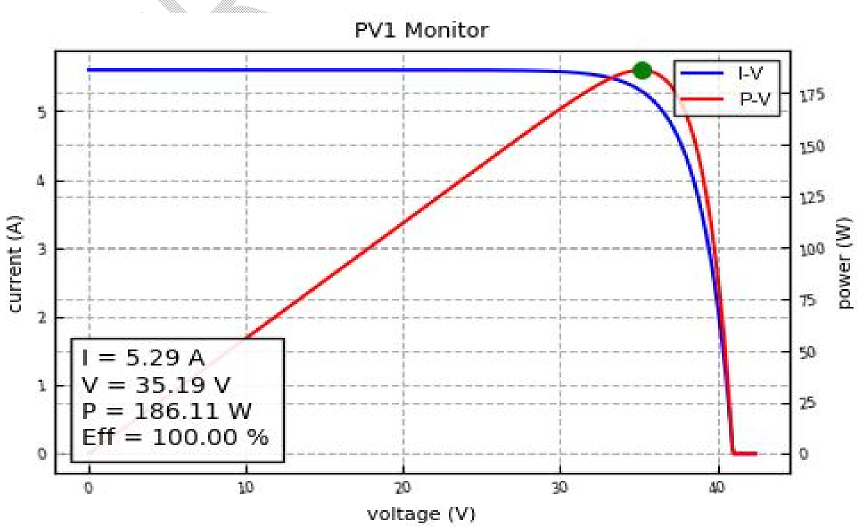

Fig 7: V-I, V-P characteristics at STC

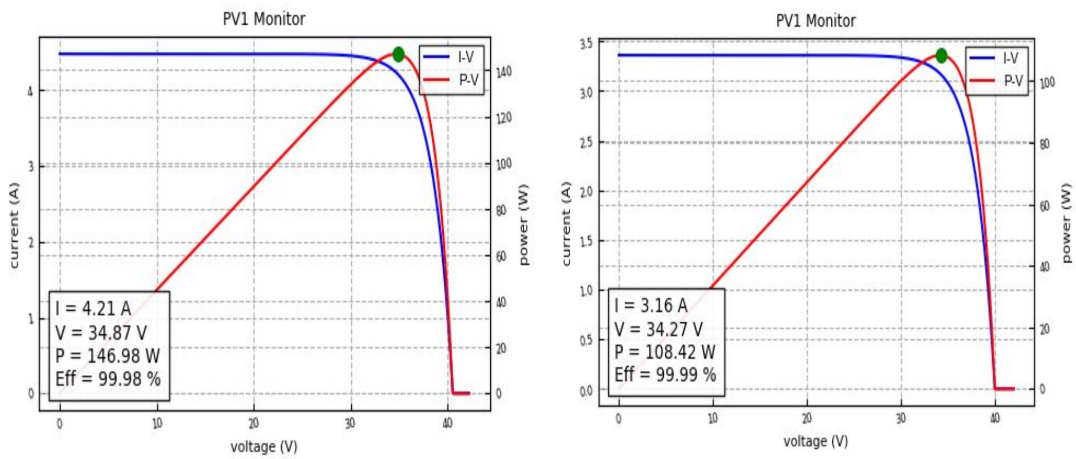

(a) (b)

Fig 8: (a) V-I, V-P characteristics for irradiation of 800 W/m^2 at 25^{0}C (b) V-I, V-P characteristics for irradiation of 600 W/m^2 at 25^{0}C.

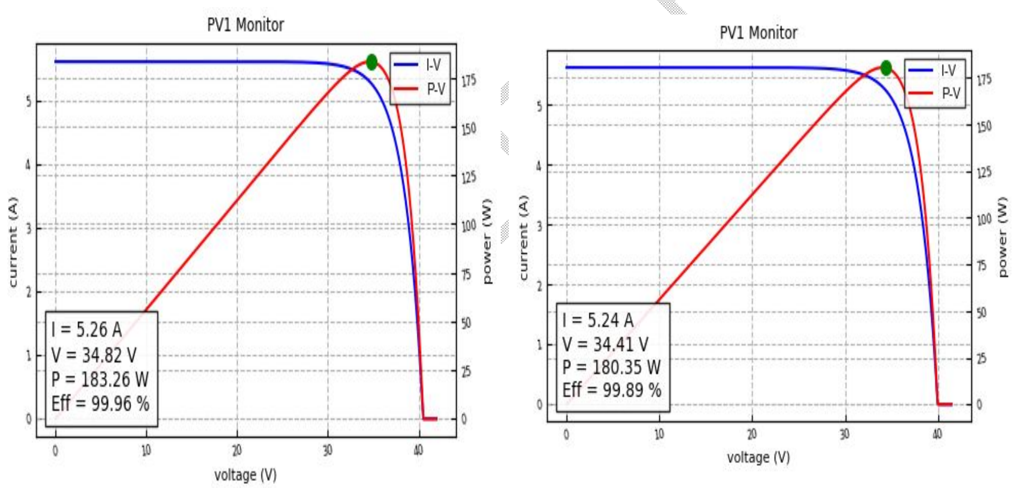

(a) (b)

Fig 9: (a) V-I, V-P characteristics for a temperature of 30^{0}C at 1000 watt/m^2 of irradiation

3.2 CHARGE / DISCHARGE MANAGEMENT

In the simulations, T = 25^{0}C is used as the reference temperature for the module. Simulation results are shown for battery management as per the flow chart shown in fig 4 during day (sunny) time when source power is more than load power. In fig 10, we can see that source power is more than load power. Fig 11,12 show the results for the case when SOC_1 is greater than or equal to 90% and when SOC_1 is below 90%. In simulations, the condition of SOC_1 below 30% is replaced by 89.98 because actually, it will take a lot of time to discharge up to 30%. Figure 13 shows that the bus voltage will be maintained at 48 V approximately at each condition.

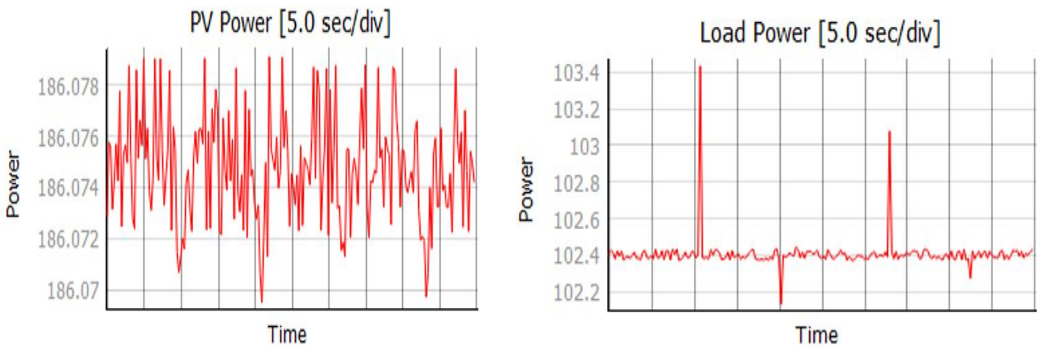

(a) (b)

Fig 10: (a) Source power (b) Load power

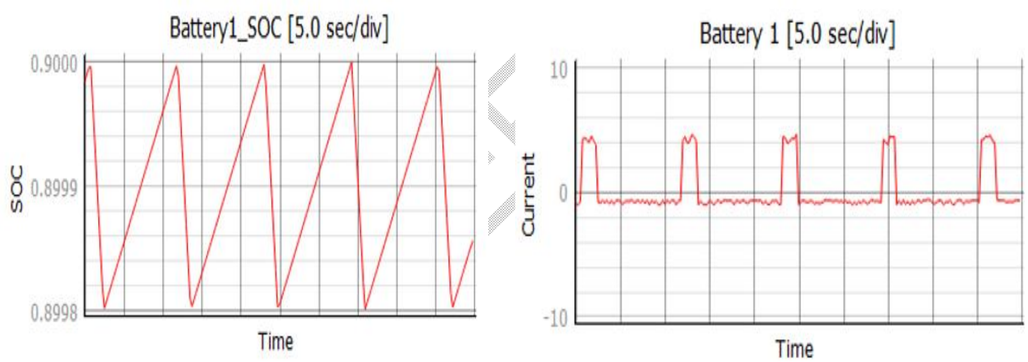

Fig 11. (a) charging discharging of battery 1 (b) flow of current in battery 1

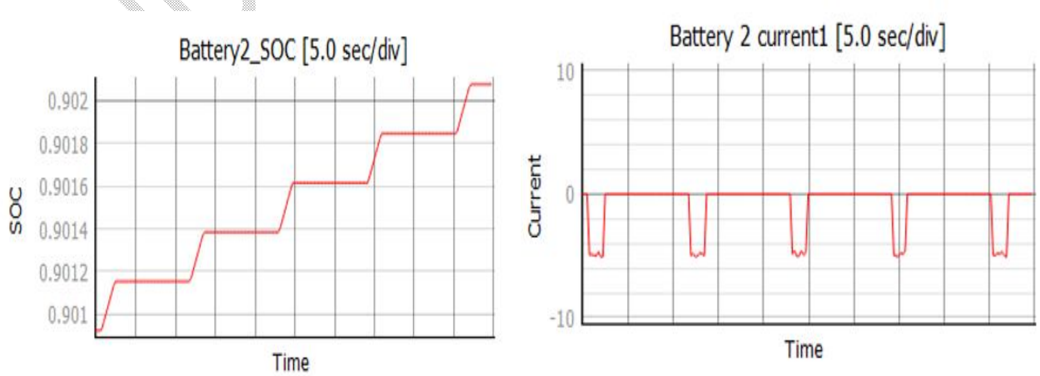

(a) (b)

Fig 6. (a) charging of battery 2 (b) flow of current in battery 2

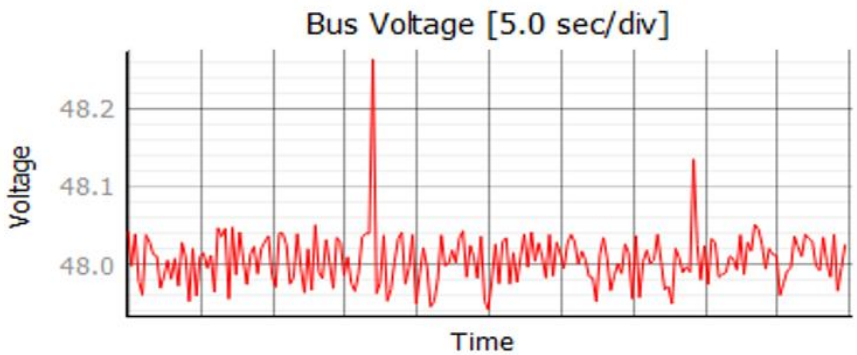

Fig 7. Bus voltage during charging/discharging of batteries

4. CONCLUSION

In this paper, a simulation of a 48V standalone DC microgrid is done using Typhoon hil software. For this, a new design of the DC MG system is used which is having a photovoltaic source connected to DC load through two batteries and DC-DC converters. By simulations, it is clear that the MPPT controller tracks maximum power at varying atmospheric conditions, batteries charge and discharge according to the algorithm used, and bus voltage is maintained at 48V. Thus, the MPPT controller and bus voltage controller remains active simultaneously with this new design and battery management system.

REFERENCES

[1] N. Ghanbari, S. Bhattacharya, and M. Mobarrez. Modeling and Stability Analysis of a DC Microgrid Employing Distributed Control Algorithm. 2018 9th IEEE Int. Symp. Power Electron. Distrib. Gener. Syst. PEDG 2018, Aug. 2018, doi: 10.1109/PEDG.2018.8447707.

[2] J. M. Guerrero, P. C. Loh, T. L. Lee, and M. Chandorkar. Advanced control architectures for intelligent microgrids Part II: Power quality, energy storage, and AC/DC microgrids. IEEE Trans. Ind. Electron 2013; 60(4): 1263–1270, doi: 10.1109/TIE.2012.2196889.

[3] H. Kakigano, Y. Miura, and T. Ise. Low-voltage bipolar-type dc microgrid for super high quality distribution. IEEE Trans. Power Electron. 2010; 25(12): 3066–3075, , doi: 10.1109/TPEL.2010.2077682.

[4] T. Dragicevic, J. M. Guerrero, J. C. Vasquez, and D. Skrlec. Supervisory control of an adaptive-droop regulated DC microgrid with battery management capability. IEEE Trans. Power Electron. 2014; 29(2): 695–706, doi: 10.1109/TPEL.2013.2257857.

[5] S. Ferahtia, A. Djeroui, H. Rezk, A. Houari, S. Zeghlache, and M. Machmoum. Optimal control and implementation of energy management strategy for a DC microgrid. Energy. Jan. 2022; 238: 121777, , doi: 10.1016/J.ENERGY.2021.121777.

[6] H. Rezk, R. M. Ghoniem, S. Ferahtia, A. Fathy, M. M. Ghoniem, and R. Alkanhel. A Comparison of Different Renewable-Based DC Microgrid Energy Management Strategies for Commercial Buildings Applications. Sustain. 2022; 14(24), doi: 10.3390/su142416656.

[7] S. Ali, Z. Zheng, M. Aillerie, J. P. Sawicki, M. C. Péra, and D. Hissel. A review of dc

microgrid energy management systems dedicated to residential applications. Energies. 2021; 14(14), 1–26, doi: 10.3390/en14144308.

[8] F. S. Al-Ismail. DC Microgrid Planning, Operation, and Control: A Comprehensive Review. IEEE Access. 2021; 9, 36154–36172, , doi: 10.1109/ACCESS.2021.3062840.

[9] K. M. Bhargavi, N. S. Jayalakshmi, D. N. Gaonkar, A. Shrivastava, and V. K. Jadoun. A comprehensive review on control techniques for power management of isolated DC microgrid system operation. IEEE Access. 2021; 9, 32196–32228, , doi: 10.1109/ACCESS.2021.3060504.

[10] M. S. Alam, F. S. Al-Ismail, F. A. Al-Sulaiman, and M. A. Abido. Energy management in DC microgrid with an efficient voltage compensation mechanism. Electr. Power Syst. Res.2022; 214,108842, 2023, doi: 10.1016/j.epsr.2022.108842.

[11] A. Jhunjhunwala, A. Lolla, and P. Kaur. Solar-dc Microgrid for Indian Homes: A Transforming Power Scenario. IEEE Electrif. Mag. 2016; 4(2):10–19, doi: 10.1109/MELE.2016.2543950.

[12] N. P. Tulasi and L. D. Aithepalli. Droop control of bi-directional DC-DC converter for improved voltage regulation and load sharing in DC microgrid. Int. J. Intell. Eng. Syst. 2019; 12(3): 228–243, doi: 10.22266/ijies2019.0630.23.

[13] C. Li, T. Dragicevic, N. L. Diaz, J. C. Vasquez, and J. M. Guerrero. Voltage scheduling droop control for State-of-Charge balance of distributed energy storage in DC microgrids. ENERGYCON 2014 - IEEE Int. Energy Conf. 2014; 1310–1314, , doi: 10.1109/ENERGYCON.2014.6850592.